retrospectively evaluated. All patients received 36.25 Gy in 5 fractions (7.25 Gy/fraction) once-weekly using 6-MV flattening filter-free photons and volumetric modulated arc therapy (VMAT). The once-weekly schedule was chosen because of the patients' comorbidity status. SBRT was delivered to the prostate gland only, without pelvic lymph-node irradiation. Before simulation, all patients underwent intraprostatic fiducial marker implantation for image-guided radiotherapy (IGRT). All patients were treated with complete-arc VMAT; beam entry through the hip prostheses was minimized using an avoidance optimization structure extending 1 cm around each implant with a dose constraint of 5 Gy. For simulation, all patients underwent a planning CT with MAR. No hydrogel rectal spacers were used. Patient positioning was verified before each fraction using cone-beam CT, with image matching based on the intraprostatic fiducial markers. No patient received androgen deprivation therapy. Acute and long-term toxicities were assessed according to the Common Terminology Criteria for Adverse Events (CTCAE). International Prostatic Symptom Score (IPSS) was used to assess baseline urinary status before SBRT. Performance status was assessed using Karnofsky Performance Status (KPS) scale. Treatment response was monitored through periodic clinical examinations and prostate-specific antigen measurements. *Results:* Six patients were available for retrospective analysis. Median age at diagnosis was 77 years (range=68-84 years). Median IPSS before the start of SBRT was 4 (range=1-7). Median KPS was 90 (range=90-100). One patient was low risk, four patients were intermediate risk, and one patient was high risk. Median follow-up was 21 months (range=8-28) (Table I). All patients responded to treatment and, at the time of this data analysis, no patient has recurred. The median acute genito-urinary (GU) toxicity was grade 0 (range=0-1). The median acute gastro-intestinal (GI) toxicity was grade 0 (range=0-1) and median long-term GU toxicity was grade 0 (range=0-1). The median long-term GI toxicity was grade 0 (range=0-1) (Table II). *Conclusion:* Despite the preliminary nature of these findings, the limited follow-up, and the potential biases associated with the retrospective design and small sample size, once-weekly prostate SBRT was feasible and well tolerated in patients with bilateral hip prostheses. No recurrences were observed during the available follow-up. The use of advanced technologies, including MAR algorithms, VMAT, and fiducial marker-based image-guided radiotherapy, is essential for minimizing uncertainties in target and organ-at-risk delineation and dose calculation. Hydrogel rectal spacers may provide additional rectal sparing in appropriately selected patients. These findings suggest that bilateral hip prostheses do not necessarily preclude prostate SBRT; however, prospective confirmation in larger cohorts is required. Alternative treatment options, including prostatectomy, should also be considered within a multidisciplinary decision-making process.

Table I. *Patients' characteristics.*

Patient n°	6
Median age (years)	77 (range=68-84)
Median IPSS	4 (range=1-7)
Median KPS	90 (range=90-100)

Table II. *Acute and late toxicities.*

Toxicity		Grade	N° of cases
Acute	GI	G0	5
		G1	1
	GU	G0	5
		G1	1
Late	GI	G0	5
		G1	1
	GU	G0	5
		G1	1

7

EXOGENOUS EXPRESSION OF WILD-TYPE AND P53 VARIANTS DIFFERENTIALLY MODULATES CELL DEATH AND HIF-1A STATUS IN KJ29 AND CAKI-2 KIDNEY CARCINOMA CELLS

Lucio Dell'Atti[1], Damiana D'Esposito[2], Ambra Sacco[2], Carmelo Ippolito[3] and Gianluca Aguiari[2]

[1]Clinica Urologica, Azienda Ospedaliero Universitaria Delle Marche, Ancona, Italy;
[2]Dipartimento Neuroscienze e Riabilitazione, Università di Ferrara, Ferrara, Italy;
[3]UOC Urologia, Arcispedale "S. Anna", Ferrara, Italy

Background/Aim: Renal cell carcinoma (RCC) accounts for approximately 2-3% of all human malignancies, with clear cell RCC (ccRCC) representing the most common histological subtype, comprising about 70-80% of cases. Currently, combinations of immune checkpoint inhibitors (ICIs), either as doublets or in association with tyrosine kinase inhibitors (TKIs), represent the preferred first-line treatment options for metastatic disease. However, the development of drug-resistance mechanisms limits treatment efficacy and patient survival. The tumor suppressor p53 is expressed at relatively low levels in ccRCC cells, although TP53 mutations are uncommon in this malignancy. This study investigated the functional effects of wild-type p53 and the naturally occurring p53 mutants R175H and R273H in ccRCC cells. *Materials and Methods:* Caki-2 and KJ29 ccRCC cells were seeded in duplicate in six-well plates and transfected with plasmids encoding wild-type (WT) or mutant (R175H and R273H) p53 for 24 h in DMEM/F12 supplemented with 1% FBS. Control cells were transfected with an irrelevant plasmid encoding the photoprotein aequorin. After transfection, cell morphology was evaluated using phase-contrast microscopy; images were acquired with a digital camera and processed using ImageJ software. Next, cells were lysed in a buffer containing 1% Triton X-100 and a cocktail of protease and phosphatase inhibitors. Following protein electrophoresis, HIF-1α and p53 expression was assessed by western blot using specific antibodies. Levels of p53 and HIF-1α were calculated as band intensity ratio between the protein of interest and β-actin. Statistical analysis was performed using GraphPad Prism software and an unpaired *t*-test. A p-value <0.05 was considered statistically significant. *Results:* KJ29 and Caki-2 cells transfected with the control plasmid (CTRL) displayed a normal morphology (Figure 1A). In contrast, expression of wild-type p53 and the R273H variant induced a marked cell detachment, with cell rounding and reduced cell volume in both ccRCC cell lines (Figure 1A). Notably, the expression of the p53 mutant R175H did not affect cell morphology, which remained comparable to CTRL cells (Figure 1A). Western blot analysis confirmed that cells transfected with p53 WT, R175H, and R273H exhibited higher levels of p53 protein than CTRL cells (Figure 1B). Interestingly, the expression of both wild-type p53 and R273H variant induced a significant down-regulation of HIF-1α compared with CTRL cells (Figure 1B). In contrast, the p53 R175H variant did not alter HIF-1α expression, showing levels comparable to those observed in CTRL cells (Figure 1B). *Conclusion*: Although p53 mutations are relatively rare in ccRCC, we have previously demonstrated that p53 expression is lower in ccRCC cells than in normal kidney cells. This suggests that p53 dysfunction may contribute to tumor development and progression in kidney cancer. In the present study, wild-type p53 and the R273H variant induced marked morphological changes consistent with reduced cell viability and significantly suppressed HIF-1α expression. In contrast, the expression of p53 R175H mutant did not affect cell morphology, which remained similar to control cells, suggesting a loss of functional activity. We also evaluated the expression of the angiogenic factor hypoxia-inducible factor 1α (HIF-1α), which is constitutively activated in most ccRCC cases. As expected, control cells exhibited elevated levels of this transcription factor, whereas cells expressing wild-type p53 and the R273H variant showed a marked reduction in HIF-1α expression. No significant changes in HIF-1α levels were observed in cells expressing the p53 R175H mutant, further supporting its loss of function. In conclusion, our findings indicate that wild-type p53 induces cell death and suppresses HIF-1α expression in ccRCC cells. Notably, the p53 R273H variant appears to retain these functional properties, whereas the R175H mutant does not exhibit antitumor activity. These results suggest that the restoration of wild-type p53 function or the reactivation of p53 mutants could represent a promising therapeutic strategy for patients with metastatic RCC.

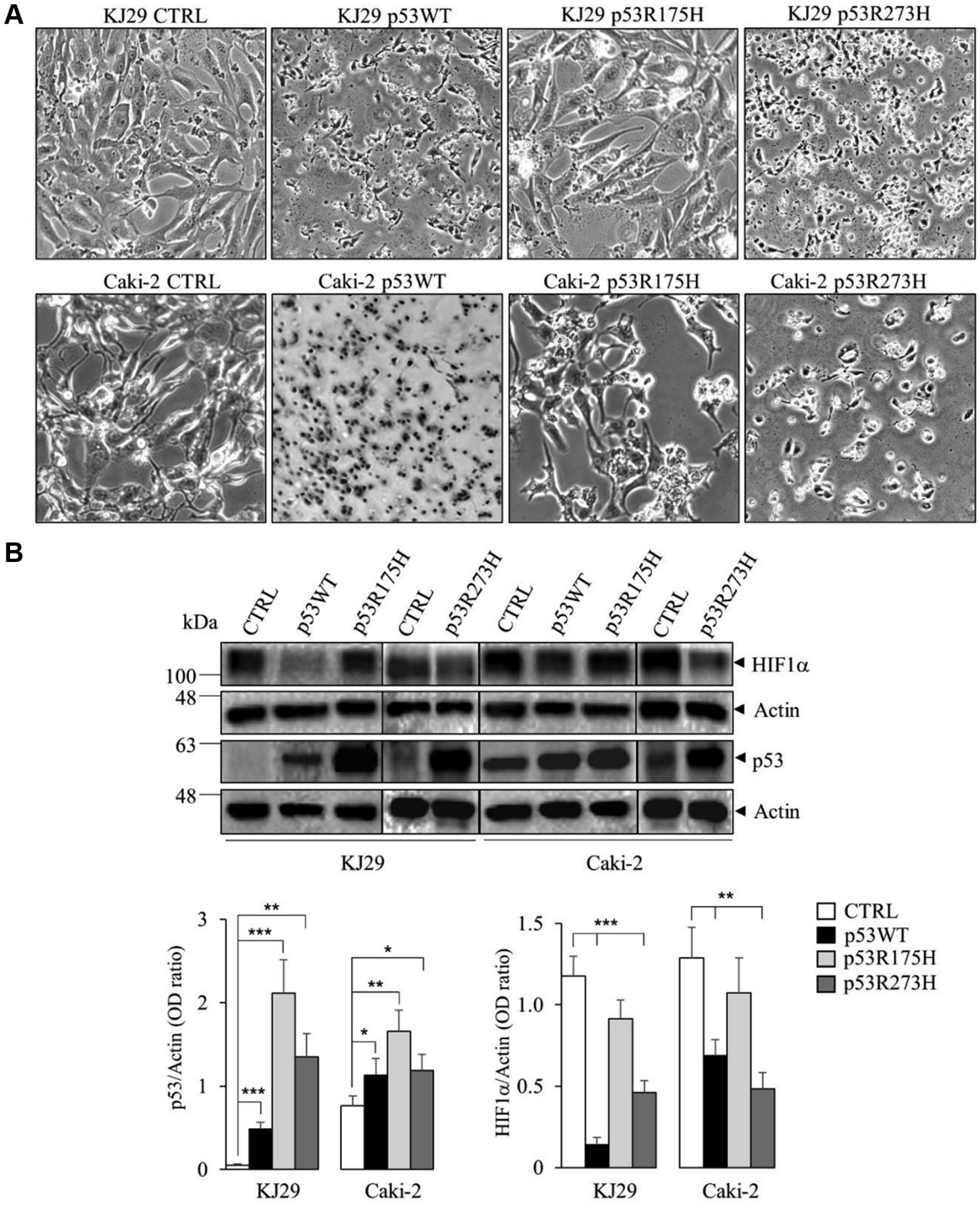


Figure 1. *Analysis of cell morphology and HIF-1α expression in clear cell renal cell carcinoma cells expressing p53 wild type (WT) and two naturally occurring variants. (A) The expression of p53WT induced marked cell death, as evidenced by extensive cell detachment in both cell lines compared with control cells (CTRL). (B) The expression of HIF-1α, p53 WT, and p53 mutants was analyzed by western blotting. Levels of wild type and mutated forms of p53 are increased in KJ29 and Caki-2 cells transfected with the corresponding plasmids compared with those transfected with the control vector (CTRL). Notably, the presence of wild type p53 strongly reduces the expression of HIF-1α in both cell lines, whereas the expression of p53 R175H variant does not affect the levels of this transcription factor.*